Simulation of High Range-Resolution Profiles of Humans Behind Walls

Shobha Sundar Ram, Craig Christianson and Hao Ling
Dept. of Electrical and Computer Engineering
University of Texas at Austin
1 University Station, Austin, TX, USA 78712

***Abstract*—In this paper, we present a technique for simulating time-varying, high range-resolution profiles of human motions behind inhomogeneous walls. This technique combines primitive based modeling of humans with wall simulation models generated using the finite difference time domain technique. Simulated range profiles of a walking human in free space and behind a reinforced concrete wall are presented.**

I. INTRODUCTION

The detection, tracking and identification of humans are topics of current interest in law enforcement and urban area military operations. Several different types of ultra-wideband (UWB) radars operating below 5GHz have been reported for this purpose [1-3]. However, tracking humans through walls remains a challenging problem since humans are non-rigid, dynamic bodies that have a wide variety of poses resulting in significant variations in their radar signatures. Also walls are complex media for wave propagation that introduce considerable distortions such as attenuation, delay and multipath to the radar returns.

There has been research undertaken to characterize the radar signatures of humans using computational electromagnetic techniques such as the finite difference time domain (FDTD) technique [4] and high-frequency ray tracing [5]. FDTD is a full-wave electromagnetic solver that yields highly accurate radar signatures of a still human. Xpatch, based on the shooting and bouncing ray technique, was also found to be satisfactory in generating human signatures. However, neither of these techniques is well suited for generating the radar signatures of dynamic human motions. These techniques require detailed computer models of humans over multiple poses and are computationally very expensive to carry out. Other simpler techniques that have been used to model human motion scattering mechanisms are the point scatterer model [6] and the primitive based prediction model [7]. In the primitive based technique, the different body parts of humans are modeled as simple shapes such as ellipsoids and spheres. The technique is fast and simple. It has been effectively combined with computer animation models of humans generated from motion capture technology (MOCAP) to simulate the radar Doppler signatures of different human motions such as walking, running, crawling and jumping [8, 9].

In this paper, we simulate the high range-resolution signatures of a moving human behind a wall by combining primitive based human modeling with wall models derived using FDTD. In Section 2, we describe the technique for simulating the human radar signatures from MOCAP data and validate the simulation model with measured data. In Section 3, we describe the inhomogeneous wall simulation model developed using FDTD. In Section 4, we combine the wall and human simulation models and show the high range-resolution radar signatures of a human behind an inhomogeneous wall.

II. HUMAN RADAR SIGNATURE SIMULATION USING MOTION CAPTURE DATA

The technique for generating human radar signatures using MOCAP data is described. The MOCAP system, at the University of Texas Virtual Reality Laboratory, consists of 16 infrared cameras that are used to locate the three-dimensional positions of 48 sensors attached at different joints on the human subject as shown in Fig. 1a. Simultaneously, Doppler radar data is collected using a 2.4GHz Doppler radar testbed [10]. As the human subject moves, the Doppler shifted radar returns are collected and processed by the short-time Fourier transform (STFT) to generate the Doppler spectrogram of the human subject as shown in Fig. 1b. Over the 18 seconds collection interval, the subject undergoes a variety of movements. The Doppler of the human is positive with the subject moving towards the radar and negative with the subject moving away from the radar. The motions of the arms and legs modulate the received signal and result in the microDoppler features that are observed in the Doppler spectrogram. The largest microDopplers come from the feet and legs.

Using the sensors location data provided by the MOCAP system, it is possible to generate an approximate model of the human skeleton structure where different bones are connected

This work is supported by the National Science Foundation under grant CBET-0730924.

978-1-4244-2871-7/09/$25.00 ©2009 IEEE

through joints. Each body part associated with the bone is modeled as an ellipsoid. The time varying radar returns of the body part is then given by (1):

$$y_b(t) = \sqrt{\sigma_b}\,\frac{1}{R^2}\,e^{-j\frac{2\pi f_c}{c}2r_b(t)} \quad (1)$$

where $r_b(t)$, R and σ_b are the time-varying phase center, range and RCS of the part and f_c is the frequency of the radar. The dielectric properties of human flesh are also incorporated in the calculation of the RCS. The radar return of the human is the complex sum of the radar returns of all the body parts. Note that shadowing and multiple interactions between the different parts are not incorporated in this model. Fig. 1c shows the resulting spectrogram from the simulated data. It is observed that the Doppler features in the spectrograms generated from measured and simulated data look very similar. This is particularly discernible in the fine Doppler features arising from the motions of the human subject's legs (for example: 6 – 10s in the Doppler spectrograms). However, there are some differences in the two spectrograms. In Fig. 1b, we observe some radio frequency interference at ± 60Hz and ± 80Hz due to the collection environment inside an office. Secondly, the simulation model appears to over estimate the RCS of the limbs in Fig. 1c. Also some of the highest Dopplers in Fig. 1b do not appear in Fig. 1c due to the fact that infrared sensors were not placed on the feet of the human subject during motion capture. Hence the 3D position data of the feet were not captured. Despite these differences, it appears that the primitive based model of humans is reasonably accurate in capturing the key radar features of a human.

III. FDTD Simulation Model of Wall

In [11, 12], simple homogeneous walls were characterized using ray optical techniques. However, their utility for modeling highly inhomogeneous walls is suspect. Here, we apply the FDTD simulation to derive the transmission loss through the wall. Since the FDTD simulation is computationally expensive, we limit the simulation to two-dimensional geometries (invariant in height). The simulation space is *1m* x *1.5m (X: -0.5m to 0.5m, Y: 0m to 1.5m)* and bounded by a perfectly matched layer (PML). A pulse source of 0.23ns duration is placed at the position (*X: 0m, Y: 0.1m*). The wall, shown in Fig. 2, is a reinforced concrete wall that is *1m* x *19.5cm (X: -0.5m to 0.5m, Y: 0.3m to 0.495m)* with a dielectric constant of 7 and conductivity 0.0498 S/m. It is reinforced by square metal conductors that are 2.25cm thick and 19.75cm apart. The simulator is run long enough so that multiple reverberations within the wall reach the end of the simulation space. The time domain electric field at every point, $\boldsymbol{r}$, in the FDTD grid space is then Fourier transformed to obtain the transfer coefficient as a function of frequency, $H(\boldsymbol{r}, f_c)$. Figs. 3a and 3b show the magnitude and phase response for a free space case (without the wall) for a carrier frequency of 2.4GHz. The magnitude response shows the electric field strength decaying as the distance from the source increases. The phase response shows a regular circular spread. Figs. 3c and 3d show the magnitude and phase response for the simulation space with the presence of the reinforced concrete wall. In the magnitude response, the wall introduces significant attenuation of the order of 2-10 dB. Also, the multiple scattering introduced by the wall's inhomogeneity interfere destructively in some regions. Likewise, distortions are also introduced in the phase response especially near the wall as seen in Fig. 3d.

IV. Simulated Time-Varying Range Profile of a Human Walking Behind a Wall

Next, we combine the primitive based human simulation with the FDTD simulation of the wall to generate the radar returns of humans behind walls. In order to constrain the movements of the simulated human to the area within the small FDTD simulation space, the translation motion of the human is removed by fixing the position of the hip joint at *(X: 0m, Y: 1m).* A radar of 2GHz *(1.4GHz to 3.4 GHz)* bandwidth is assumed to be located at *(X: 0m, Y: 0.1m).* The human is modeled according to the primitive based prediction technique described in Section 2. However while computing the radar returns from each body part of the human, the free space wave propagation factor of equation (1) is replaced by the two-way wall transfer coefficient generated from the FDTD simulation. This is shown in (2):

$$y_b(t, f_c) = \sqrt{\sigma_b}\left\{H[r_b, f_c]\right\}^2 \quad (2)$$

Since the FDTD simulation model is two dimensional, the transfer coefficient was scaled to correspond to the transfer function that would be generated from a three dimensional simulation model. The radar return of the human, $y(t, f_c)$, generated by the sum of the radar returns from all N body parts, is a function of both the frequency of the radar and time. The time-varying radar range profile, $Y(t, R)$ is generated by inverse Fourier transforming $y(t, f_c)$ along the f_c dimension:

$$Y(t, R) = \int \sum_{b=1}^{N} y_b(t, f_c)\, e^{+j\frac{2\pi f_c}{c}2R}\, df_c \quad (3)$$

Figs. 4a and 4b show the time-varying range profiles of a walking human, at bore sight with respect to the radar, for both the free space case and when the human is behind the reinforced concrete wall. The range resolution is 7.5cm. The MOCAP data for the walking motion was obtained from Sony Computer Entertainment America. Since the translation motion is suppressed, the range of the human torso remains fixed at 0.9m for free space as seen in Fig. 4a. Due to the periodic motion of the limbs, the ranges of the limbs fluctuate between 0.4m to 1.2m. The feet undergo the maximum displacement. In Fig. 4b, the signal strength is attenuated by about 10dB. Also, the wall introduces a delay in the transmission response. Hence the range of the torso appears to shift to 1.2m. Similarly, the ranges of all the other body parts are also shifted by approximately 0.3m. The multiple bounces of the wave within the wall, give rise to late-time ringing in

the range profiles. Thus the presence of multipath appears to introduce a significant distortion on the range profiles of the human walking motion.

V. Conclusion

In this paper, we have presented a technique for modeling dynamic human radar signatures behind complex, inhomogeneous walls. First, we validated the primitive based modeling of humans by simultaneously generating radar data and MOCAP data of complex human motions. Second, we combined the primitive based human simulation with FDTD simulation of the wall to generate the radar returns of humans behind walls. The radar range profiles of a human in free space were compared with the radar range profiles of a human behind a reinforced concrete wall.

Acknowledgment

We are grateful to Prof. Dana Ballard and Mr. Rahul Iyer of the Virtual Reality Laboratory, Dept. of Computer Science, the University of Texas at Austin, for providing us access to the motion capture data collection.

References

[1] S. Nag, H. Fluhler and M. Barnes, "Preliminary interferometric images of moving targets using a time modulated using ultra wideband through-wall penetration radar, " *IEEE Radar Conf.,* pp. 64 – 69, May 2001.

[2] G. Franceschetti, J. Tatoian, D. Giri and G. Gibbs, "Timed arrays and their application to impulse SAR for through-the-wall imaging," *IEEE Antennas Propagat. Soc. Int. Symp. Digest,* vol. 3, pp. 3067 – 3070, June 2004.

[3] R. M. Narayanan, "Through-wall radar imaging using UWB noise waveforms," *J. Franklin Inst*., vol. 346, no. 6, pp. 659 – 678, July 2008.

[4] T. Dogaru and L. Nguyen, "FDTD models of electromagnetic scattering by the human body," *IEEE Antennas Propagat. Soc. Int. Symp. Digest,* pp. 1995 – 1998, July 2006.

[5] T. Dogaru and C. Le, "Validation of Xpatch computer models for human body radar signature," ARL-TR-4403, March 2008.

[6] J. L. Geisheimer, E. F. Greneker and W. S. Marshall, "High-resolution Doppler model of the human gait," *SPIE Proc. Radar Sensor Tech. Data Vis.*, vol. 4744, pp. 8 – 18, July 2002.

[7] P. van Dorp and F. C. A. Groen, "Human walking estimation with radar," *IEE Proc. Radar Sonar Navigation*, vol. 150, pp. 356 – 365, Oct. 2003.

[8] S. S. Ram and H. Ling, "Simulation of human microDopplers using computer animation data," *IEEE Radar Conf.* May 2008.

[9] S. S. Ram and H. Ling, "MicroDoppler signature simulation of computer animated human and animal motions," *IEEE Antennas Propagat. Soc. Int. Symp. Digest,* July 2008.

[10] A. Lin and H. Ling, "Doppler and direction-of-arrival radar for multiple mover sensing," *IEEE Trans. Aerospace and Electronic Systems*, vol. 43, pp. 1496 – 1509, Oct 2007.

[11] T. B. Gibson and J. C. Jenn, "Prediction and measurement of wall insertion loss," *IEEE Trans. Antennas Propagat.*, vol. 47, pp. 55 – 57, Jan. 1999.

[12] M. Dehmollaian and K. Sarabandi, "Refocusing through building walls using synthetic aperture radar," *IEEE Trans. Geoscience and Remote Sensing* vol. 46, pp. 1589 – 1599, June 2008.

[13] C. Christianson, 'Through-wall radar propagation study using the finite difference time domain method' M.S. thesis, The University of Texas at Austin, May 2008.

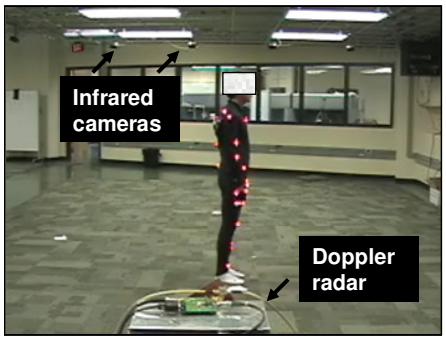

(a)

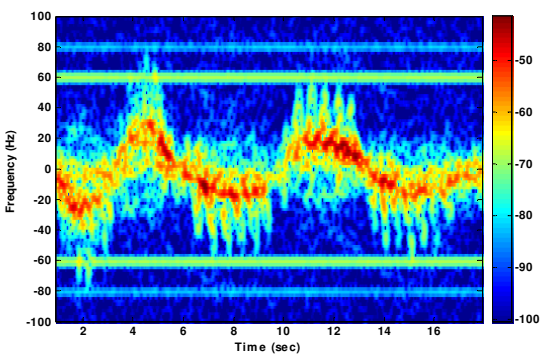

(b)

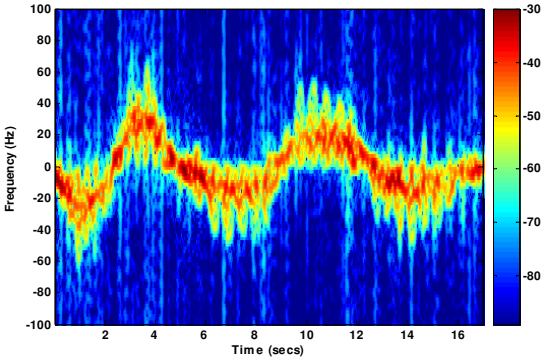

(c)

Fig. 1(a) Simultaneous generation of infrared motion capture data and Doppler radar data of a moving human subject. (b) Doppler spectrogram of human motions at 2.4GHz generated from measured Doppler radar data, (c) Simulated Doppler spectrogram of human motions at 2.4GHz generated from motion capture data and primitive based model of human.

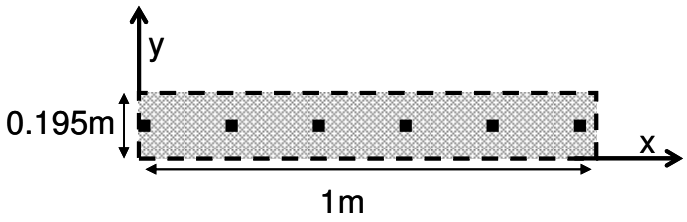

Fig. 2: FDTD simulation model of a reinforced concrete wall

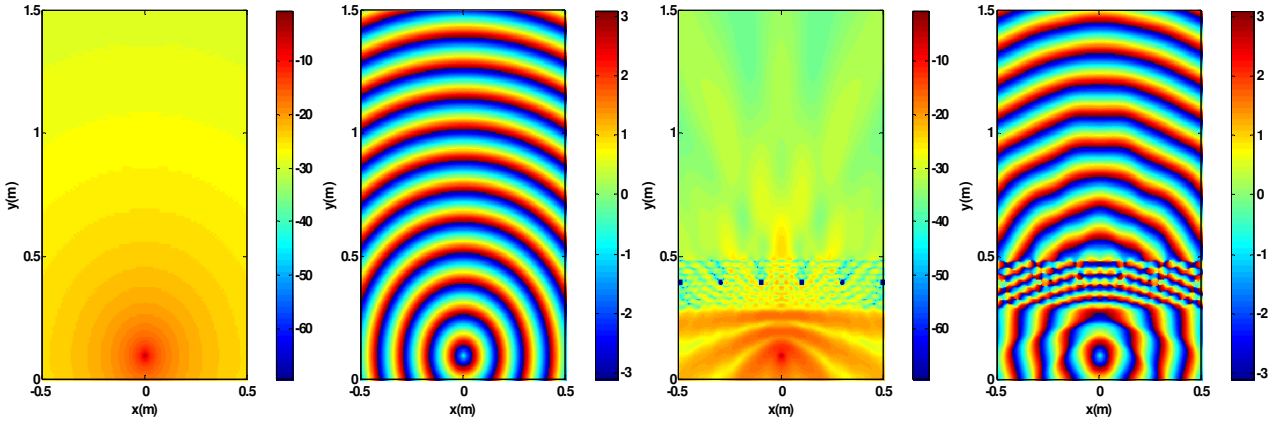

(a) (b) (c) (d)

Fig. 3(a) Magnitude response for free space at 2.4GHz, (b) Phase response for free space at 2.4 GHz, (c) Magnitude response for reinforced concrete wall case at 2.4 GHz and (d) Phase response for reinforced concrete wall case at 2.4GHz.

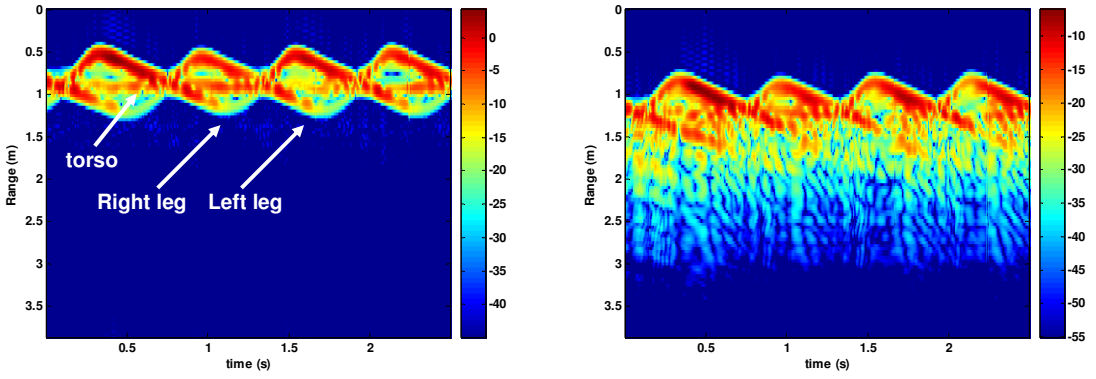

(a) (b)

Fig. 4. Simulated range profile of a walking human in (a) free space and (b) behind a reinforced concrete wall.